Naval Research Laboratory

Washington, DC 20375-5320

NRL/MR/6750--13-9489

Finite Larmor Radius and Collisional Effects on the Electron-Ion Hybrid Instability

E.M. Tejero
G. Ganguli
C. Crabtree
W.E. Amatucci

Charged Particle Physics Branch
Plasma Physics Division

V. Sotnikov

Air Force Research Laboratory
Dayton, Ohio

C.L. Enloe

Air Force Academy
Colorado Springs, Colorado

November 18, 2013

REPORT DOCUMENTATION PAGE

Form Approved
OMB No. 0704-0188

1. REPORT DATE *(DD-MM-YYYY)*	**2. REPORT TYPE**	**3. DATES COVERED** *(From - To)*
18-11-2013	Memorandum Report	

4. TITLE AND SUBTITLE

Finite Larmor Radius and Collisional Effects on the Electron-Ion Hybrid Instability

5a. CONTRACT NUMBER

5b. GRANT NUMBER

5c. PROGRAM ELEMENT NUMBER

6. AUTHOR(S)

E.M. Tejero, V. Sotnikov,[1] G. Ganguli, C. Crabtree, W.E. Amatucci, and C.L. Enloe[2]

5d. PROJECT NUMBER
67-9872-03 & 67-4774-02

5e. TASK NUMBER

5f. WORK UNIT NUMBER

7. PERFORMING ORGANIZATION NAME(S) AND ADDRESS(ES)

Naval Research Laboratory
4555 Overlook Avenue, SW
Washington, DC 20375-5320

8. PERFORMING ORGANIZATION REPORT NUMBER

NRL/MR/6750--13-9489

9. SPONSORING / MONITORING AGENCY NAME(S) AND ADDRESS(ES)

Office of Naval Research
One Liberty Center
875 North Randolph Street, Suite 1425
Arlington, VA 22203-1995

Air Force Office of Scientific Research
875 North Randolph Street, Suite 325, Rm. 3112
Arlington, VA 22203-1768

10. SPONSOR / MONITOR'S ACRONYM(S)

ONR & AFOSR

11. SPONSOR / MONITOR'S REPORT NUMBER(S)

12. DISTRIBUTION / AVAILABILITY STATEMENT

Approved for public release; distribution is unlimited.

13. SUPPLEMENTARY NOTES

[1]Air Force Research Laboratory, Dayton, OH
[2]Air Force Academy, Colorado Springs, CO

14. ABSTRACT

The Electron-Ion Hybrid instability, a transverse velocity shear-driven instability with frequency near the lower hybrid frequency, has been observed theoretically and experimentally. It was shown previously that the scale length of the gradient in the velocity must be much smaller than the ion gyroradius and larger than the electron gyroradius in order to generate the short wavelength electron-ion hybrid mode. In this paper, the original theory for the electron-ion hybrid instability has been extended to include finite gyroradius radius effects and electron-neutral collisions with the intention of applying this theory to the plasma region surrounding hypersonic vehicles. In this plasma layer, these sorts of transverse sheared flows can exist in a collisional plasma. While this dense layer of plasma can itself impede communications, the density structures created by the lower hybrid turbulence can also be a source of scattering for these electromagnetic signals.

15. SUBJECT TERMS

16. SECURITY CLASSIFICATION OF:			**17. LIMITATION OF ABSTRACT**	**18. NUMBER OF PAGES**	**19a. NAME OF RESPONSIBLE PERSON**
a. REPORT	**b. ABSTRACT**	**c. THIS PAGE**			Erik M. Tejero
Unclassified Unlimited	Unclassified Unlimited	Unclassified Unlimited	Unclassified Unlimited	11	**19b. TELEPHONE NUMBER** *(include area code)* (202) 767-3215

Standard Form 298 (Rev. 8-98)
Prescribed by ANSI Std. Z39.18

I. INTRODUCTION

Over the past twenty years, there have been numerous studies both theoretical[1–9] and experimental[10–15] into the destabilizing effects of inhomogeneous electric fields transverse to the ambient magnetic field. It has been demonstrated that the electric field gradient scale length L_E is the key length scale that determines the nature of the instability[16]. If L_E is on the order of the ion gyroradius ρ_i, then the instability will be driven by the dynamics of the ions and could be an electrostatic ion cyclotron wave or an Alfvén wave depending on the plasma β[15]. However, if $\rho_e \ll L_E < \rho_i$, then the ions do not $\mathbf{E} \times \mathbf{B}$ drift and the instability will be driven by the dynamics of the electrons. These waves are primarily electrostatic lower hybrid waves in the VLF range. All of these velocity shear-driven instabilities are primarily azimuthally propagating in the direction of the $\mathbf{E} \times \mathbf{B}$ drift.

In this report, we will focus on the electron-ion hybrid instability (EIH), which is observed in the case where $\rho_e \ll L_E < \rho_i$. This case has been studied in relation to boundary layer conditions in the plasma sheet and in laser generated plasmas, where lower hybrid waves have been observed in environments with sharp electric field gradients that are required for the instability. We want to extend this work to include the plasma environment created around hypersonic vehicles. Depending on the speed of the vehicle, the plasma densities can become quite large such that the plasma can cutoff any communications signals to and from the vehicle. However, we are interested in densities below the point where communication blackout occurs. The plasma layer that is created also has a velocity profile due to motion of the vehicle through the neutral medium. This sheared plasma flow can give rise to similar instabilities to those described above. These plasma instabilities in their nonlinearly saturated state can form coherent density structures that can also disrupt communication signals. It is these nonlinear structures and their effects on electromagnetic radiation that we wish to study. To that end, we will extend the EIH theory to include finite electron-neutral collisions and finite larmor radius effects to include important facets of the hypersonic vehicle plasma environment.

Manuscript approved September 10, 2013.

II. THEORY

In order to extend the existing theory for the EIH instability, we start the derivation from the fluid equations for a species α with no temperature gradient:

$$\frac{\partial n_\alpha}{\partial t} + \nabla \cdot (n_\alpha \mathbf{v}_\alpha) = 0, \tag{1}$$

$$\frac{\partial \mathbf{v}_\alpha}{\partial t} + (\mathbf{v}_\alpha \cdot \nabla)\, \mathbf{v}_\alpha = \frac{q_\alpha}{m_\alpha} (\mathbf{E} + \mathbf{v}_\alpha \times \mathbf{B}) - \nu_{\alpha n} (\mathbf{v}_\alpha - \mathbf{v}_n) - \frac{T_\alpha}{m_\alpha n_\alpha} \nabla n_\alpha. \tag{2}$$

We linearize the equations assuming $A \sim A_0 + A_1(x) \exp[i(k_y y + k_z z - \omega t)] + ...$ higher order terms that we neglect. We take the inhomogeneity to be in the $\hat{x}$ direction: $\mathbf{E} = E_0(x)\hat{x} + \mathbf{E}_1$, the magnetic field to be $\mathbf{B} = B_0 \hat{z}$, and the equilibrium drift along $\mathbf{v}_{0\alpha} = v_{0\alpha}\hat{y}$.

From the continuity equation to first order, we arrive at the following expressions:

$$n_{1\alpha} = \frac{n_0}{\omega_{1\alpha}} \left(-i \frac{\partial v_{1\alpha x}}{\partial x} + k_y v_{1\alpha y} + k_z v_{1\alpha z} \right), \tag{3}$$

where we have assumed that the equilibrium electron and ion densities are uniform and equal to n_0 and defined $\omega_{1\alpha} = \omega - k_y v_{0\alpha}$.

From the momentum equation to first order, we arrive at the following expression:

$$v_{1\alpha x} = \frac{i}{D_\alpha} \left(k_y \Omega_\alpha - \hat{\omega}_\alpha \frac{\partial}{\partial x} \right) \left(\frac{q_\alpha}{m_\alpha} \phi_1 + \frac{v_{t\alpha}^2}{n_0} n_{1\alpha} \right), \tag{4}$$

$$v_{1\alpha y} = \frac{1}{D_\alpha} \left(k_y \hat{\omega}_\alpha - \eta_\alpha \Omega_\alpha \frac{\partial}{\partial x} \right) \left(\frac{q_\alpha}{m_\alpha} \phi_1 + \frac{v_{t\alpha}^2}{n_0} n_{1\alpha} \right), \text{ and} \tag{5}$$

$$v_{1\alpha z} = \frac{k_z}{\hat{\omega}_\alpha} \left(\frac{q_\alpha}{m_\alpha} \phi_1 + \frac{v_{t\alpha}^2}{n_0} n_{1\alpha} \right), \tag{6}$$

where we have defined $D_\alpha = \hat{\omega}_\alpha^2 - \eta_\alpha \Omega_\alpha^2$, $\hat{\omega}_\alpha = \omega_{1\alpha} + i\nu_{\alpha n}$, $\eta_\alpha = 1 + \frac{1}{\Omega_\alpha} \frac{\partial v_{0\alpha}}{\partial x}$, $\Omega_\alpha = \frac{q_\alpha B_0}{m_\alpha}$, and $v_{t\alpha}^2 = \frac{T_\alpha}{m_\alpha}$.

Substituting Equations (4-6) into Equation (3), we can write a general expression for the perturbed density for a species α.

$$\begin{aligned} &\left[1 + \frac{v_{t\alpha}^2}{D_\alpha} \frac{\hat{\omega}_\alpha}{\omega_{1\alpha}} \left\{ D_\alpha \frac{\partial}{\partial x} \left(\frac{1}{D_\alpha} \frac{\partial}{\partial x} \right) - k_y^2 + \frac{k_y \Omega_\alpha}{\hat{\omega}_\alpha D_\alpha} \frac{\partial D_\alpha}{\partial x} - \frac{k_z^2 D_\alpha}{\hat{\omega}_\alpha^2} \right\} \right] n_{1\alpha} \\ &= -\frac{q_\alpha n_0}{m_\alpha D_\alpha} \frac{\hat{\omega}_\alpha}{\omega_{1\alpha}} \left[D_\alpha \frac{\partial}{\partial x} \left(\frac{1}{D_\alpha} \frac{\partial}{\partial x} \right) - k_y^2 + \frac{k_y \Omega_\alpha}{\hat{\omega}_\alpha D_\alpha} \frac{\partial D_\alpha}{\partial x} - \frac{k_z^2 D_\alpha}{\hat{\omega}_\alpha^2} \right] \phi_1 \end{aligned} \tag{7}$$

We assume that the ions are an unmagnetized cold fluid and that ion-neutral collisions can be ignored. These assumptions imply that the ions do not $\mathbf{E} \times \mathbf{B}$ drift $\mathbf{v}_{0i} = 0$, $\eta_i = 1$,

$\omega_{1i} = \omega$, $\nu_{in} = 0$, and $T_i = 0$. In addition, the frequency of interest ω is near the lower hybrid frequency such that $\Omega_e \gg \omega \gg \Omega_i$. This implies that $D_i \approx \omega^2$. Under these assumptions, we can rewrite Equation (7) for the ions as:

$$n_{1i} = -\frac{en_0}{m_i\omega^2}\left[\frac{\partial^2}{\partial x^2} - k_y^2 - k_z^2\right]\phi_1. \tag{8}$$

The electrons are taken to be a warm magnetized fluid, and we keep the electron-neutral collision frequency. The electrons $\mathbf{E}\times\mathbf{B}$ drift at $\mathbf{v}_{0e} = v_E = -\frac{E}{B_0}$. As for the ions we treat the frequency such that $\Omega_e \gg \omega \gg \Omega_i$, which implies that $D_e \approx= -\eta_e\Omega_e^2$. We also consider these equations in the small shear limit such that $\frac{1}{\Omega_e}\frac{\partial v_E}{\partial x} \ll 1$. Under these assumptions, we can rewrite Equation (7) for the electrons as:

$$\begin{aligned}\left[1 - \rho_e^2\frac{\hat{\omega}_e}{\omega_{1e}}\left\{\frac{\partial^2}{\partial x^2} - k_y^2 + \frac{k_y}{\hat{\omega}_e}\frac{\partial^2 v_E}{\partial x^2} + \frac{k_z^2\Omega_e^2}{\hat{\omega}_e^2}\right\}\right]n_{1e} = -\frac{en_0}{m_e\Omega_e^2}\frac{\hat{\omega}_e}{\omega_{1e}}\times \\ \left[\frac{\partial^2}{\partial x^2} - k_y^2 + \frac{k_y}{\hat{\omega}_e}\frac{\partial^2 v_E}{\partial x^2} + \frac{k_z^2\Omega_e^2}{\hat{\omega}_e^2}\right]\phi_1.\end{aligned} \tag{9}$$

The partial x derivative has a scale size equal to the electric field gradient scale length L_E. Since $\rho_e \ll L_E < \rho_i$, which is why the electrons $\mathbf{E}\times\mathbf{B}$ drift and the ions do not, we can drop the second derivative of n_{1e} since it goes like ρ_e^2/L_E^2. This leads to the following expression for the perturbed electron density:

$$n_{1e} \approx -\frac{en_0}{m_e\Omega_e^2}\left[\left(1-\rho_e^2\kappa^2\right)\left(1 + i\frac{\nu_{en}}{\omega_{1e}}\right)\left(\frac{\partial^2}{\partial x^2} - k_y^2\right) + \frac{k_y}{\omega_{1e}}\frac{\partial^2 v_E}{\partial x^2} + \frac{k_z^2\Omega_e^2}{\omega_{1e}^2 + i\nu_{en}\omega_{1e}}\right]\phi_1, \tag{10}$$

where $\kappa^2 = \left(1 + i\frac{\nu_{en}}{\omega_{1e}}\right)\left(k_y^2 - \frac{k_y}{\omega_{1e}+i\nu_{en}}\frac{\partial^2 v_E}{\partial x^2} - \frac{k_z^2\Omega_e^2}{(\omega_{1e}+i\nu_{en})^2}\right)$.

We substitute Equation (8) and Equation (10) into Poisson's equation, $\nabla^2\phi_1 + \frac{e}{\epsilon_0}n_{1i} - \frac{e}{\epsilon_0}n_{1e} = 0$, and after a mess of algebra, we arrive at:

$$\begin{aligned}&\left[\omega^2\left(1 - \frac{1}{2}R^2\left\{k_y^2 - \frac{k_y}{\omega_{1e}}\frac{\partial^2 v_E}{\partial x^2}\right\}\right) - \omega_{LH}^2 + i\frac{\nu_{en}}{\omega_{1e}}\left\{\omega^2\left(\frac{1+2\delta^2}{1+\delta^2} + i\frac{\nu_{en}}{\omega_{1e}}\frac{\delta^2}{1+\delta^2}\right)\right.\right. \\ &\left.\left. - \omega_{LH}^2\right\}\right]\left(\frac{\partial^2}{\partial x^2} - k_y^2\right)\phi_1 + \omega^2\left(1 + i\frac{\nu_{en}}{\omega_{1e}}\right)\frac{\delta^2}{1+\delta^2}\frac{k_y}{\omega_{1e}}\frac{\partial^2 v_E}{\partial x^2}\phi_1 + \omega^2 M\frac{\omega_{LH}^2}{\omega_{1e}^2}k_z^2\phi_1 = 0,\end{aligned} \tag{11}$$

where $\delta = \omega_{pe}/\Omega_e$, $R^2 = 2\delta^2\rho_e^2/(1+\delta^2)$, $M = m_i/m_e$ and we have ignored terms with factors of $\nu_{en}R^2$.

III. NUMERICAL SOLUTIONS

Equation (11) is an eigenvalue equation that can be solved numerically for the wave potential profile and the complex eigenvalue ω. We can rewrite Equation (11) using normalized

quantitites as follows:

$$\frac{\partial^2 \phi_1}{\partial \bar{x}^2} - Q\left(\bar{x}, \bar{\omega}\right) \phi_1 = 0, \tag{12}$$

where we have defined Q as

$$Q\left(\bar{x}, \bar{\omega}\right) = \bar{k}_y^2 - \frac{\bar{\omega}^2}{F}\left[\frac{M\bar{k}_z^2}{\bar{\omega}_{1e}^2} + \frac{\delta^2}{1+\delta^2}\left(1 + i\frac{\bar{\nu}_{en}}{\bar{\omega}_{1e}}\right)\frac{\bar{k}_y}{\bar{\omega}_{1e}}\frac{\partial^2 \bar{v}_E}{\partial \bar{x}^2}\right] \tag{13}$$

and we have used the lower hybrid frequency ω_{LH} and the electric field scale length L_E to define our characteristic time and length scales for the normalized quantities, e.g. $\bar{k}_y = k_y L_E$ and $\bar{\omega} = \omega/\omega_{LH}$. It follows that the characteristic velocity scale is $\omega_{LH} L_E$ such that $\bar{v}_E = v_E/(\omega_{LH} L_E)$. It should also be noted that

$$F = \bar{\omega}^2\left[1 - \frac{1}{2}\bar{R}^2\left(\bar{k}_y^2 - \frac{\bar{k}_y}{\bar{\omega}_{1e}}\frac{\partial^2 \bar{v}_E}{\partial \bar{x}^2}\right)\right] - 1 + i\frac{\bar{\nu}_{en}}{\bar{\omega}_{1e}}\left[\bar{\omega}^2\left(\frac{1+2\delta^2}{1+\delta^2} + i\frac{\bar{\nu}_{en}}{\bar{\omega}_{1e}}\frac{\delta^2}{1+\delta^2}\right) - 1\right]. \tag{14}$$

For our numerical calculations, we will be using the following expression for R^2 that is derived from a kinetic treatment[17] instead of the expression determined in the previous section from the fluid approximation:

$$R^2 = \begin{cases} 3\lambda_{Di}^2, & \text{for } \Omega_e \gg \omega_{pe} \\ \dfrac{3}{4}\rho_e^2 + 3\rho_i^2, & \text{for } \Omega_e \ll \omega_{pe} \end{cases} \tag{15}$$

where the ion Debye length is $\lambda_{Di}^2 = T_i/(4\pi n e^2)$.

If we consider large $\bar{x}$ values, where we can take $\bar{v}_E$ and its derivatives to be zero, Equation (13) has no spatial dependence and Equation (12) can be immediately solved to yield:

$$\phi_1\left(\bar{x}\right) = A\exp\left(\bar{k}_x \bar{x}\right) + B\exp\left(-\bar{k}_x \bar{x}\right), \tag{16}$$

where $\bar{k}_x = \pm\sqrt{Q\left(\bar{x} \to \pm\infty, \bar{\omega}\right)}$. To start, we choose the same electric field profile used in Ganguli, Lee, and Palmadesso[2]:

$$\mathbf{E}\left(\bar{x}\right) = \frac{E_0}{\cosh^2\left(\bar{x}\right)}\hat{\bar{x}}. \tag{17}$$

We use a standard numerical shooting code[18] to solve Equation (12). Using the asymptotic solution given in Equation (16), we start the the numerical integration with a purely decaying solution for a large negative value of $\bar{x}$ for a given guess for $\bar{\omega}$. We determine the values of the coefficients, A and B, from the result of the numerical integration for a large positive value of $\bar{x}$. We adjust $\bar{\omega}$ to minimize the coefficient in front of the growing asymptotic solution. Figure (1) (a) shows the real (solid black line) and imaginary (dashed red

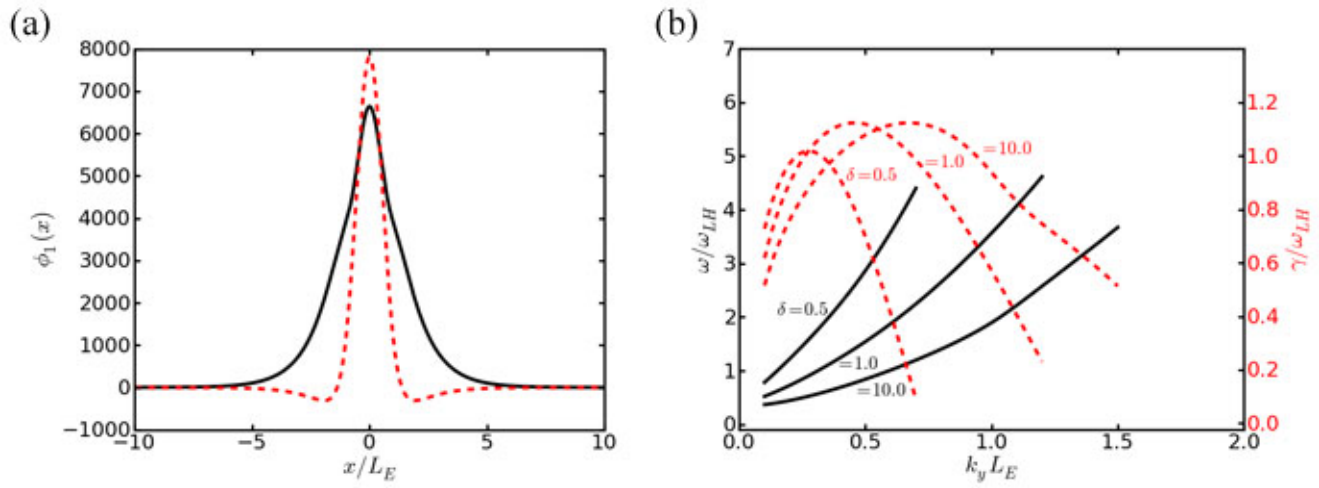

FIG. 1. Plot (a) shows the real (solid black line) and imaginary (dashed red line) parts of a typical eigenfunction solution of (12) with $k_yL_E = 1.0$, $\delta = 10.0$, $\alpha = 0.l$, and $\omega = (1.9 + 0.94i)\omega_{LH}$. Plot (b) shows profiles of the real frequency (solid black lines) and growth rate (dashed red lines) as functions of k_yL_E for three different values of δ.

line) parts of a typical eigenfunction solution of (12) for the following parameters: $\bar{k}_y = 1.0$, $\bar{k}_z = 0$, $\delta = 10.0$, $\bar{v}_E = 0.1005$, $M = 1833$, $\bar{\nu}_{en} = 0$, and $\bar{\rho}_e = 0$. The resulting complex eigenvalue is $\omega = (1.9 + 0.94i)\omega_{LH}$. Figure (1) (b) shows profiles of the real frequency (solid black lines) and growth rate (dashed red lines) as functions of $\bar{k}_y$ for three different values of δ. These results are consistent with figures in the Ganguli, Lee, and Palmadesso paper[2], which were determined for similar parameters. With these benchmarks for the shooting code, we can now look at how $\bar{\nu}_{en}$ and $\bar{\rho}_e$ effect these solutions.

IV. DISCUSSION

The plasma environment near hypersonic vehicles can be highly collisional, so we wish to investigate the effects of neutral collisions on the electron-ion hybrid instability. Since the ions are already considered as being unmagnetized, the effects of ion-neutral collisions will be minimal, and consequently we ignored them in the above derivation. The frequency of the EIH instability tends to be near the lower hybrid frequency though it can be Doppler-shifted significantly due to the presence of the nonuniform electron flows. We expect to

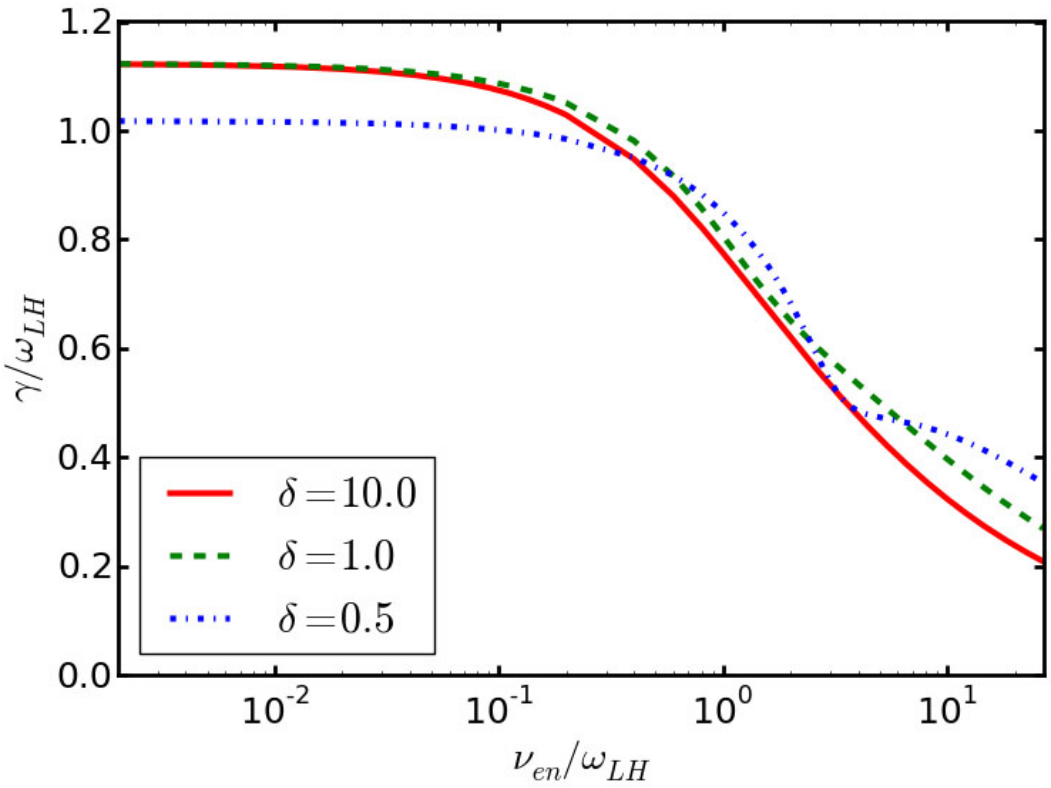

FIG. 2. Plot shows the growth rate as a function of normalized electron-neutral collision frequency for three values of δ and the same conditions used in Figure (1b).

start to see the effects of the electron-neutral collisions when $\nu_{en} \approx \omega_{LH}$. Due to the drift approximation that we made in the above derivation, there is an upper limit to the collision frequency we can study with Equation (12), $\nu_{en} < 0.1\ \Omega_e$ such that $\nu_{en}/\Omega_e \ll 1$. Figure (2) shows typical profiles of growth rate as a function of the electron-neutral collision frequency normalized to the lower hybrid frequency for the same three values of δ used in Figure (1b), where the range of the abscissa is $[10^{-5}\ \Omega_e,\ 0.1\ \Omega_e]$. As can be seen there is a sudden drop in the growth rate for the three curves, but the plasma is not completely stabilized by electron-neutral collisions. The critical values where collisional effects become important are dependent on the value of δ: for $\delta = 10.0 \Rightarrow \nu_{en} = 0.22\ \omega_{LH}$, $\delta = 1.0 \Rightarrow \nu_{en} = 0.22\ \omega_{LH}$, and $\delta = 0.5 \Rightarrow \nu_{en} = 1.35\ \omega_{LH}$.

We seek to investigate the nonlinear saturation of this instability. Specifically, we wish to study the formation of coherent stationary structures that result from the nonlinear

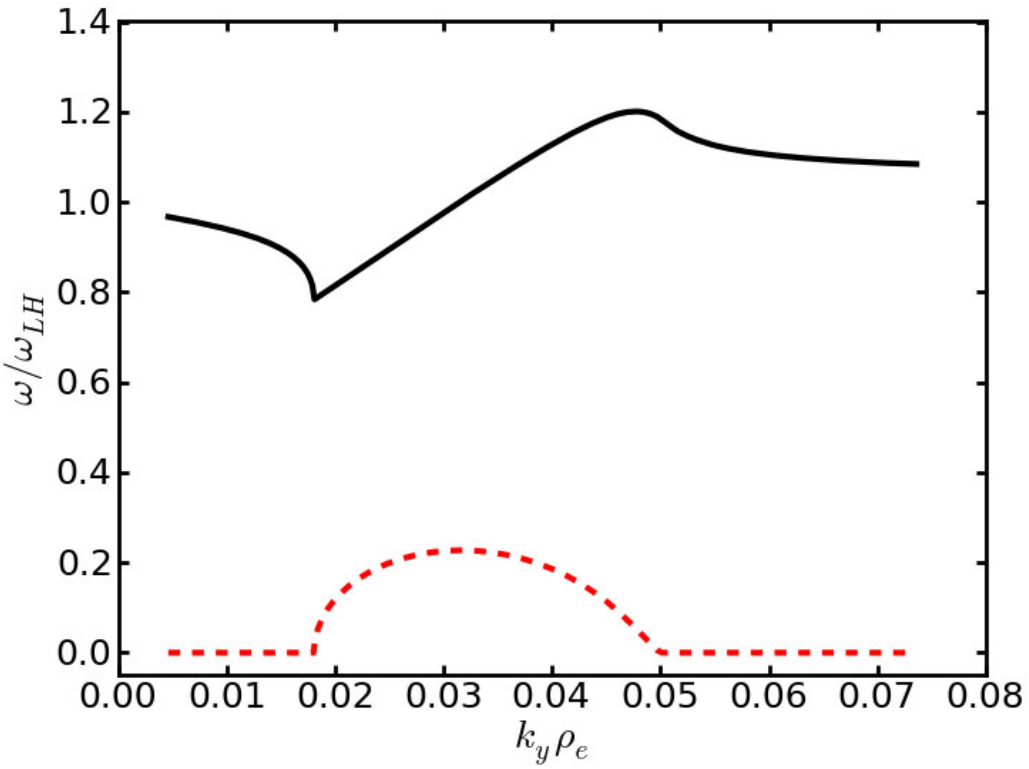

FIG. 3. Plot shows profiles of real frequency (solid black line) and growth rate (dashed red line) as functions of $k_y\rho_e$. These profiles were calculated using the following parameters: $\delta = 0.35$, $\mu = 40.0$, $\alpha = 0.002$, $\bar{k}_z = \bar{\nu}_{en} = 0$, and $\bar{\rho}_e = 0.046$.

coupling of the instability in the lower hybrid range and ion acoustic waves by means of the modulation instability. In order to have this nonlinear pathway be dominant, we search for solutions that are centered around the lower hybrid frequency and that have unstable solutions for a narrow range of $k_y\rho_e$. Figure (3) shows profiles of real frequency (solid black line) and growth rate (dashed red line) as functions of $k_y\rho_e$. These profiles were calculated using the following parameters: $\delta = 0.35$, $\mu = 40.0$, $\alpha = 0.002$, $\bar{k}_z = \bar{\nu}_{en} = 0$, and $\bar{\rho}_e = 0.046$. For these conditions, the unstable solutions are centered in a small range around the lower hybrid frequency and occur in a narrow range of $k_y\rho_e$. In future studies, the following nonlinear equations from Sotnikov et al.[19] will be solved to investigate the development of

the nonlinear coherent stationary structures:

$$\begin{aligned}\frac{\partial^2}{\partial t^2}\left[\left(1+\frac{1}{2}R^2\nabla^2\right)\hat{L}_1^2\nabla^2\phi_1+M\omega_{LH}^2\frac{\partial^2\phi_1}{\partial z^2}-\frac{\delta^2}{1+\delta^2}\hat{L}_1\frac{\partial^2 v_E}{\partial x^2}\frac{\partial\phi_1}{\partial y}\right]\\ +\omega_{LH}^2\hat{L}_1^2\nabla^2\phi_1=\frac{\delta^2}{1+\delta^2}\frac{\partial^2}{\partial t^2}\hat{L}_1\left\{\frac{\delta n}{n_0},\phi_1\right\}\end{aligned} \tag{18}$$

$$\frac{\partial^2\delta n}{\partial t^2}-\left(v_{ti}^2+v_s^2\right)\nabla^2\delta n=-\frac{i}{4\pi M}\frac{\omega_{pe}^2}{\Omega_e\omega_{LH}}\nabla^2\left\{\phi_1,\phi_1^*\right\}, \tag{19}$$

where we have used the following definitions

$$\{a,b\}=\frac{\partial a}{\partial x}\frac{\partial b}{\partial y}-\frac{\partial a}{\partial y}\frac{\partial b}{\partial x}\qquad\text{and}\qquad\hat{L}_1=\frac{\partial}{\partial t}+v_E\left(x\right)\frac{\partial}{\partial y}.$$

V. CONCLUSION

We have extended the work of Ganguli et al. for the electron-ion hybrid in order to include important effects for the plasma environment surrounding a hypersonic vehicle and written the necessary shooting code to solve this new system. We have shown that the instability is robust; the effects of electron-neutral collisions take effect when $\nu_{en}\approx\omega_{LH}$. However, even electron-neutral collision frequencies near 0.1 Ω_e do not fully stabilize the plasma, and above this threshold the notion of an $\mathbf{E}\times\mathbf{B}$ drift is no longer valid. With finite larmor radius effects included, we have obtained an operating range where we can look for the development of nonlinear stationary structures due to the nonlinear coupling of the unstable shear-driven lower hybrid mode and low frequency ion acoustic waves.

VI. ACKNOWLEDGEMENTS

This work is supported by the Naval Research Laboratory base program and the Air Force Office of Scientific Research (AFOSR).

REFERENCES

[1]G. Ganguli, Y. C. Lee, and P. Palmadesso, Phys. Fluids **28**, 761 (1985).

[2]G. Ganguli, Y. C. Lee, and P. Palmadesso, Phys. Fluids **31**, 2753 (1988).

[3]G. Ganguli, Y. C. Lee, and P. J. Palmadesso, Phys. Fluids **31**, 823 (1988).

[4]K.-I. Nishikawa, G. Ganguli, Y. C. Lee, and P. J. Palmadesso, Phys. Fluids **31**, 1568 (1988).

[5]H. Romero and G. Ganguli, Phys. Fluids B **5**, 3163 (1993).

[6]J. R. Peñano, G. Ganguli, W. E. Amatucci, D. N. Walker, and V. Gavrishchaka, Phys. Plasmas **5**, 4377 (1998).

[7]J. R. Peñano and G. Ganguli, Phys. Rev. Lett. **83**, 1343 (1999).

[8]J. R. Peñano and G. Ganguli, J. Geophys. Res. **105**, 7441 (2000).

[9]J. R. Peñano and G. Ganguli, J. Geophys. Res. **107**, 1189 (2002).

[10]M. E. Koepke, W. E. Amatucci, J. J. Carroll III, and T. E. Sheridan, Phys. Rev. Lett. **72**, 3355 (1994).

[11]W. E. Amatucci, M. E. Koepke, J. J. Carroll III, and T. E. Sheridan, Geophys. Res. Lett. **21**, 1595 (1994).

[12]M. E. Koepke, W. E. Amatucci, J. J. Carroll III, V. Gavrishchaka, and G. Ganguli, Phys. Plasmas **2**, 2523 (1995).

[13]W. E. Amatucci, D. N. Walker, G. Ganguli, J. A. Antoniades, D. Duncan, J. H. Bowles, V. Gavrishchaka, and M. E. Koepke, Phys. Rev. Lett. **77**, 1978 (1996).

[14]E. Thomas, Jr., J. D. Jackson, E. A. Wallace, and G. Ganguli, Phys. Plasmas **10**, 1191 (2003).

[15]E. M. Tejero, W. E. Amatucci, G. Ganguli, C. D. Cothran, C. Crabtree, and E. Thomas, Jr., Phys. Rev. Lett. **106**, 185001 (2011).

[16]G. Ganguli, M. J. Keskinen, H. Romero, R. Heelis, T. Moore, and C. Pollock, J. Geophys. Res. **99**, 8873 (1994).

[17]V. Sotnikov, V. D. Shapiro, and V. I. Shevchenko, Sov. J. Plasma Phys. **4**, 252 (1978).

[18]W. H. Press, S. A. Teukolsky, W. T. Vetterling, and B. P. Flannery, *Numerical Recipes*, 3rd ed. (Cambridge University Press, New York, NY, 2007).

[19]V. Sotnikov, T. Kim, E. Mishin, W. E. Amatucci, G. Ganguli, E. Tejero, T. A. Mehlhorn, and I. Paraschiv, Proceedings from AMOS 2012 Conference (2012).